Modeling Of Self-Consistent Electric Fields In Tokamak Edge Plasma With B2.5 Code

V. Rozhansky*, S. Voskoboynikov*, E. Kovaltsova*, D. Coster**, R. Schneider**

**St.Petersburg State Technical University, 195251 St.Petersburg, Russia*
*** Max-Planck Institut fur Plasmaphysik, Euroatom Association, Garching, Germany*

Introduction

An important issue of self-consistent electric fields in the edge tokamak plasma has been addressed by many authors. Electric fields in the scrape-off layer (SOL) cause $\vec{E}\times\vec{B}$ drifts which result in a redistribution of the plasma and impurity density between the divertor legs. Radial electric field in the vicinity of a separatrix is responsible for the transition into improved confinement regime (L-H transition). The 2D problem of calculation of self-consistent electric field is rather complicated since it is necessary to perform calculations both on open and closed field lines, while electric field is determined by various mechanisms of perpendicular conductivity. In this paper results of full simulation of the problem by means of B2.5 transport code are presented for the parameters of ASDEX-Upgrade tokamak. The calculations are performed for the single fluid case (deuterium) and typical Ohmic discharge. All important mechanisms of the transverse conductivity have been taken into account. The fluid equations have been transformed to exclude the divergence free part of diamagnetic and viscosity-driven drifts, heat fluxes and currents. Relative role of different mechanisms of the transverse conductivity has been studied. It is demonstrated that diamagnetic currents and perpendicular currents caused by classical parallel ion viscosity are responsible for the potential distribution in the vicinity of the separatrix.

Basic equations

Standard Braginskii fluid equations were solved with anomalous values of diffusion and heat conductivity coefficients. The part of diamagnetic velocity, which is not divergence free and remains after cancellation in the particle, parallel momentum and energy balance equations, has been taken in the form (*x*, *y*, *z* are the poloidal, radial and toroidal directions):

$$V_{\perp}^{(dia)} = \frac{T_i B}{e}\frac{\partial}{h_y \partial y}\left(\frac{1}{B^2}\right), \quad V_y^{(dia)} = -\frac{T_i B_z}{e}\frac{\partial}{h_x \partial x}\left(\frac{1}{B^2}\right). \tag{1}$$

Current continuity equation has been solved

$$\frac{1}{\sqrt{g}}\frac{\partial}{\partial x}\left(\frac{\sqrt{g}}{h_x} j_x\right) + \frac{1}{\sqrt{g}}\frac{\partial}{\partial y}\left(\frac{\sqrt{g}}{h_y} j_y\right) = 0\,, \tag{2}$$

where

$$j_x = (B_z / B) j_{\perp} + (B_x / B) j_{\parallel},$$

$$\vec{j} = \vec{j}_{\parallel} + \vec{j}^{(dia)} + \vec{j}^{(vis\|)} + \vec{j}^{(AN)}, \tag{3}$$

$$j_{||} = \sigma_{||}\left[\frac{B_x / B}{e}\frac{1}{h_x}\left(\frac{1}{n}\frac{\partial nT_e}{\partial x} + 0.71\frac{\partial T_e}{\partial x}\right) - \frac{B_x / B}{h_x}\frac{\partial \varphi}{\partial x}\right]. \quad (4)$$

The non-divergence free parts of diamagnetic and viscosity-driven currents are

$$j_{\perp}^{(dia)} = \frac{n(T_e + T_i)B}{h_y}\frac{\partial}{\partial y}\left(\frac{1}{B^2}\right), \qquad j_y^{(dia)} = -\frac{n(T_e + T_i)B_z}{h_x}\frac{\partial}{\partial x}\left(\frac{1}{B^2}\right) \quad (5)$$

$$j_{\perp}^{(vis||)} = -\frac{B_x\eta_0}{3B^{1/2}}\frac{\partial\left(V_{||}B^{1/2}\right)}{h_x\partial x}\frac{\partial}{h_y\partial y}\left(\frac{1}{B^2}\right), \qquad j_y^{(vis||)} = \frac{B_x B_z\eta_0}{3B^{3/2}}\frac{\partial\left(V_{||}B^{1/2}\right)}{h_x\partial x}\frac{\partial}{h_x\partial x}\left(\frac{1}{B^2}\right). \quad (6)$$

Parallel viscosity caused by ion parallel heat flux will be added in the forthcoming publications. The anomalous current was taken in the form

$$\vec{j}^{(AN)} = -\sigma^{(AN)}\nabla\varphi, \qquad \sigma^{(AN)} = k^{(AN)}en, \qquad k^{(AN)} = 3\cdot 10^{-6} - 10^{-5}. \quad (7)$$

Such low values of $\sigma^{(AN)}$ on the one hand provide the convergence of the numerical scheme, and on the other hand does not influence the final result. It should be noted that anomalous conductivity in the form of Eq.(7) does not exist in the presence of turbulence, in contrast to diffusion or heat conductivity, due to ambipolar nature of Coulomb collisions (see for example [1]). The indirect influence of anomalous transport is connected with anomalous transport of momentum due to inertia and viscosity terms.

Results

The non-divergence free part of diamagnetic currents (which correspond to the particle guiding center vertical currents) are the largest perpendicular currents. On the closed flux surfaces far from separatrix these currents should be closed by the parallel Pfirsch-Schlueter currents

$$j_{||} = j_{||}^{P.S.} = \frac{\partial p}{h_y\partial y}\frac{B_z}{B_x B}\left(1 - \frac{B^2}{B_0^2}\right). \quad (8)$$

This is demonstrated by Fig.1. Parallel currents on the open field lines are the combination of Pfirsch-Schlueter currents and parallel thermal currents, Fig.2. Potential radial profile on the closed flux surfaces and in SOL in the vicinity of a separatrix is determined by the value of effective transverse conductivity. This is illustrated by Fig.3 which corresponds to the absence of viscosity driven currents, $\vec{E}\times\vec{B}$ drifts and diamagnetic particle fluxes. Electric field on the closed flux surfaces is, roughly speaking, inversely proportional to $\sigma^{(AN)}$. This can be understood because the averaged over the flux surface diamagnetic current in this variant is balanced by the radial anomalous current. Potential profile in SOL far from separatrix is rather insensitive to the value of $\sigma^{(AN)}$ and is determined by the electron parallel momentum balance.

For small $\sigma^{(AN)}$ the diamagnetic current should be balanced by radial current driven by parallel viscosity. The final radial potential profile is rather sensitive to the subtle structure of the pressure distribution over the flux surface, which determine the average diamagnetic current. Therefore, $\vec{E}\times\vec{B}$ drifts and diamagnetic fluxes strongly effect the result. The final result is independent on $\sigma^{(AN)}$ value and is shown in Fig.4. In Fig.5 the potential profile is compared with the neoclassical value. The results of calculations can contribute to understanding of the mechanisms of the edge transport barrier formation.

The perpendicular conductivity caused by ion-neutral collisions was inserted into the code and did not give significant contribution to the perpendicular current, and hence did not change noticeably the potential profile. Poloidal $\vec{E}\times\vec{B}$ drifts are directed from the inner to the outer divertor plate in SOL and from outer to inner plate in the private region. In the considered regime $\vec{E}\times\vec{B}$ drifts did not result in significant redistribution of density and temperature in SOL. However, they can in principle significantly influence the impurity fluxes. Our results differs from similar calculations [2], where perpendicular current driven by anomalous viscosity was taken into account. We consider larger perpendicular current driven by parallel viscosity. Our calculations provide smooth transition to the results of neoclassical theory while moving towards the core, see, for example, [3].

Acknowledgments. This work was performed according to WTZ project RUS-561-98.

References

[1] F. L. Hinton, Y.-B. Kim Nuclear Fusion **34** 899 (1994).
[2] T. D. Ronglien, D. D. Ryutov, N. Mattor, Czech. Journ. Phys. **48** Suppl. S2 201 (1998).
[3] V. Rozhansky , M. Tendler in Reviews of Plasma Phys. Ed. by B.B. Kadomtsev, Consultants Bureau N.Y.-London **19** 147 (1996).

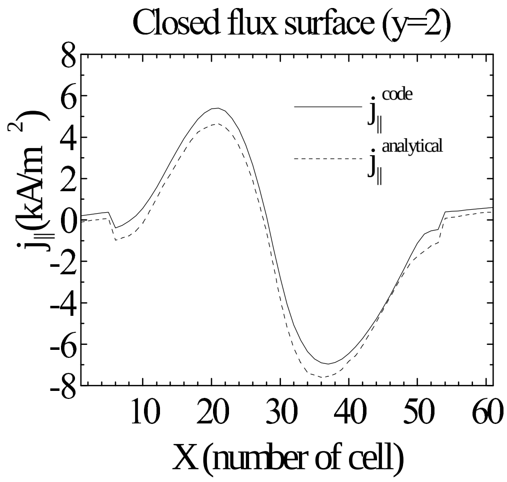

Fig. 1. Parallel current on the closed flux surface as a function of the poloidal coordinate.

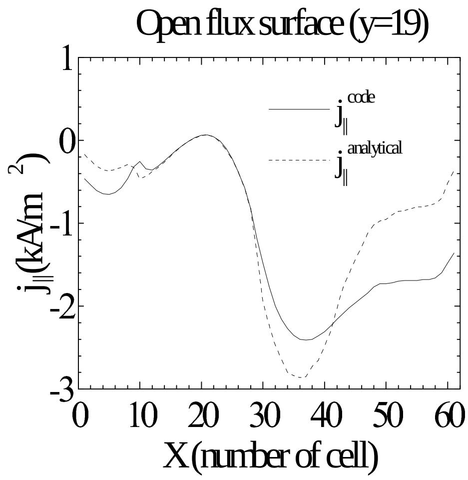

Fig. 2. Parallel current on the open field lines as a function of the poloidal coordinate.

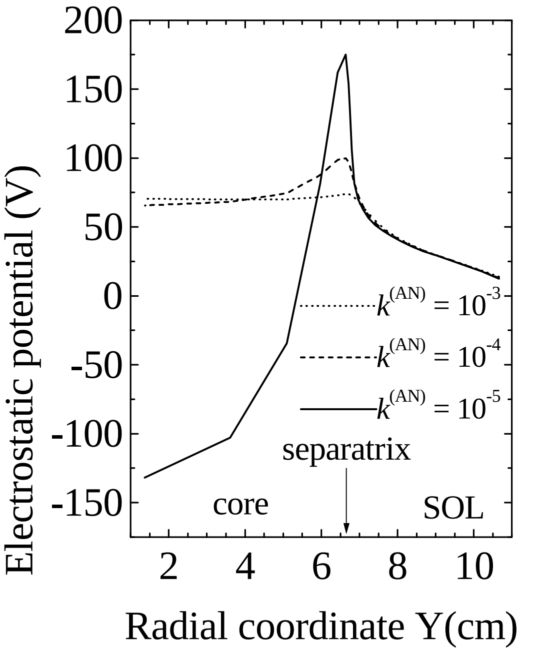

Fig. 3. Potential profile at the outer midplane (x=55). The anomalous perpendicular conductivity $\sigma^{(AN)}$ balances the diamagnetic current. The viscosity-driven current and electric drift are switched off.

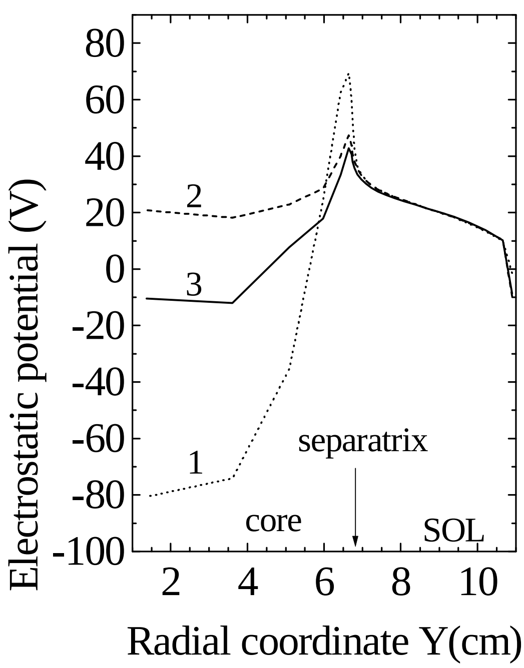

Fig. 4. Potential profiles at the outer midplane (x=55), $k^{(AN)}=10^{-5}$, viscosity-driven current is taken into account. ***1*** *- electric drifts and diamagnetic particle fluxes are switched off,* ***2*** *- electric drifts are switched on,* ***3*** *- all drifts and fluxes are switched on.*

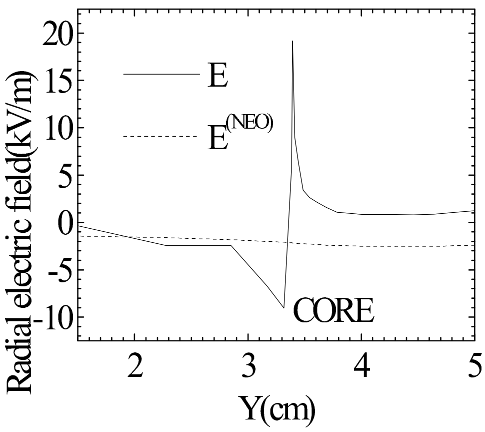

Fig. 5. Radial component of electric field E at the outer midplane (X=55) and the neoclassic electric field.